Journal of Microscopy, Vol. 212, Pt 3 December 2003, pp. 280–291
Received 30 May 2003; accepted 1 June 2003

The nacre protein perlucin nucleates growth of calcium carbonate crystals

S. BLANK*, M. ARNOLDI*[1], S. KHOSHNAVAZ*, L. TRECCANI*, M. KUNTZ†, K. MANN‡, G. GRATHWOHL† & M. FRITZ*†

**Institut für Biophysik, FB01 der Universität Bremen, Postfach 330440, 28334 Bremen, Germany*

†Institut für Keramische Werkstoffe und Bauteile, FB04 der Universität Bremen, Postfach 330440, 28334 Bremen, Germany

‡Max-Planck-Institut für Biochemie, Am Klopferspitz 18, 82152 Martinsried, Germany

Key words. Aragonite, atomic force microscopy in aqueous solution, biogenic polymer/mineral composite, biomineralization, calcite, *Haliotis laevigata*, nacre, perlucin.

Summary

Atomic force microscopy (AFM) in aqueous solution was used to investigate native nacre of the marine snail *Haliotis laevigata* on the microscopic scale and the interaction of purified nacre proteins with calcium carbonate crystals on the nanoscopic scale. These investigations were controlled by scanning electron microscopy (SEM), light microscopy (LM) and biochemical methods. For investigations with AFM and SEM, nacre was cleaved parallel to the aragonite tablets in this biogenic polymer/mineral composite. Multilamellar organic sheets consisting of a core of chitin with layers of proteins attached on both sides lay between the aragonite layers consisting of confluent aragonite tablets. Cleavage appeared to occur between the aragonite tablet layer and the protein layer. AFM images revealed a honeycomb-like structure to the organic material with a diameter of the 'honeycombs' equalling that of the aragonite tablets. The walls of the structures consisted of filaments, which were suggested to be collagen. The flat regions of the honeycomb-like structures exhibited a hole with a diameter of more than 100 nm. When incubated in saturated calcium carbonate solution, aragonite needles with perfect vertical orientation grew on the proteinacous surface. After treatment with proteinase K, no growth of orientated aragonite needles was detected. Direct AFM measurements on dissolving and growing calcite crystals revealed a surface structure with straight steps the number of which decreased with crystal growth. When the purified nacre protein perlucin was added to the growth solution (a super-saturated calcium carbonate solution) new layers were nucleated and the number of steps increased. Anion exchange chromatography of the water-soluble proteins revealed a mixture of about 10 different proteins. When this mixture was dialysed against saturated calcium carbonate solution and sodium chloride, calcium carbonate crystals precipitated together with perlucin leaving the other proteins in the supernatant. Thus perlucin was shown to be a protein able to nucleate calcium carbonate layers on calcite surfaces, and in the presence of sodium chloride, is incorporated as an intracrystalline protein into calcium carbonate crystals.

Correspondence to: Dr Habil Monika Fritz, at Institut für Biophysik. Tel.: +49 (0)421 218 3458; fax: +49 (0)421 218 2974; e-mail: mfritz@uni-bremen.de

[1]Present address: Bayrische Landesbank, Brienner Str. 18, 80333 München, Germany.

Introduction

Nacre, the lustreous layer of the molluscan shell, is a fascinating biogenic composite material with extraordinary physical properties. It combines a high mechanical strength similar to many ceramics, with elasticity, reducing the brittleness of the shell (Evans *et al.*, 2001; Wang *et al.*, 2001). The molluscan shell consists of more than 95% calcium carbonate, which is present as calcite in the outer prismatic layer and as aragonite in the inner nacreous layer (mother of pearl; Zaremba *et al.*, 1996; Weiner & Addadi, 1997; Fritz & Morse, 1998). The unique properties of nacre seem to be due to the low amount of organic matrix (1–5% by weight), which consists of proteins, glycoproteins and chitin (Zentz *et al.*, 2001; Weiss *et al.*, 2002). Thus the energy required to fracture nacre is about three orders of magnitude higher than that for pure aragonite (Currey, 1980). According to a central tenet in biomineralization, proteins and other organic polymers play an important role in the temporal and spatial control of crystal nucleation and growth (Addadi & Weiner, 1985; Borbas *et al.*, 1991;

© 2003 The Royal Microscopical Society

Berman *et al.*, 1993). A specific role is attributed to soluble polyanionic proteins as calcium-binding molecules. Partial amino acid sequences have led to the suggestion that some of these proteins have a β-sheet with a spacing of anionic side chains similar to the spacing of calcium ions in calcium carbonate crystals (Moradian-Oldak *et al.*, 1992; Morse *et al.*, 1993).

Because nacre has characteristics and resulting mechanical properties of a polymer/mineral composite, it has attracted much interest in many disciplines such colloidal physics, surface chemistry, molecular biology and material sciences. Owing to its well-organized structure nacre might also be a model system to characterize biogenic composites in general (Treccani *et al.*, 2003).

Mature nacre consists of pseudo hexagonal or polygonal aragonite tablets about 15 µm in diameter (*a*- and *b*-directions) and 0.5 µm in height (*c*-direction; Erben, 1974; Nakahara, 1983; Fritz *et al.*, 1994). The mature tablets form horizontal confluent layers that are stacked together in the vertical direction. At the growth front they appear as 'stacks of coins', where the next layer of aragonite tablets is nucleated, when the underlying one is not yet confluent (Fig. 1A,B). The layers are flat with a highly orientated crystal structure (Fritz & Morse, 1998). In most gastropods the growth front of nacre is reminiscent of 'stacks of coins' (Wada & Fujinuki, 1976). Each aragonite layer is separated by an interlamellar sheet of organic material and each tablet is surrounded by a 'box' of organic matrix (Fig. 1A,B). Organic matrix is also present in the aragonite tablets themselves, the so-called 'intracrystalline proteins' (Belcher *et al.*, 1996). The interlamellar sheets are multilamellar and consist of a water-insoluble chitin core (Weiner & Traub, 1980; Weiss *et al.*, 2002), which is sandwiched between two layers of water-insoluble proteins. Adsorbed to this surface are water-soluble proteins (Weiner, 1979; Cariolou & Morse, 1988; Schäffer *et al.*, 1997).

The growth of nacre is a fascinating example of self-organization in nature. The crystal grows far from any cell and thus also far from the genetic apparatus of the mantle epithelium, which secrets the molecular material for the shell. The molecules forming the organic sheets are thought to be deposited from the mantle epithelium and the inorganic ions and organic polymers are then secreted to fill this mould. The mechanism responsible for the highly ordered and highly coherent nature of the crystal through hundreds of layers is as yet unclear. The model for heteroepitaxial nucleation suggests that nucleation and growth of each aragonite tablet are determined by the organic sheet below. This requires a new discrete nucleation of the next aragonite layer on each succeeding organic layer. A more recent model prefers the uninterrupted growth of the crystal through mineral bridges. This is supported by the discovery of small pores in the horizontal sheets (Nakahara *et al.*, 1982; Schäffer *et al.*, 1997). Recent studies demonstrate that crystal growth is also guided by co-operative interaction with proteins in solution. Polyanionic proteins purified either from the calcitic or aragonite layer and attached to an insoluble support induce exactly the polymorph from which they were isolated (Belcher *et al.*, 1996; Falini *et al.*, 1996). These results demonstrate several mechanisms that are likely to control, in concert, the growth of nacre (Treccani *et al.*, 2003).

However, to understand the molecular details of biomineralization, characterization and functional tests of purified

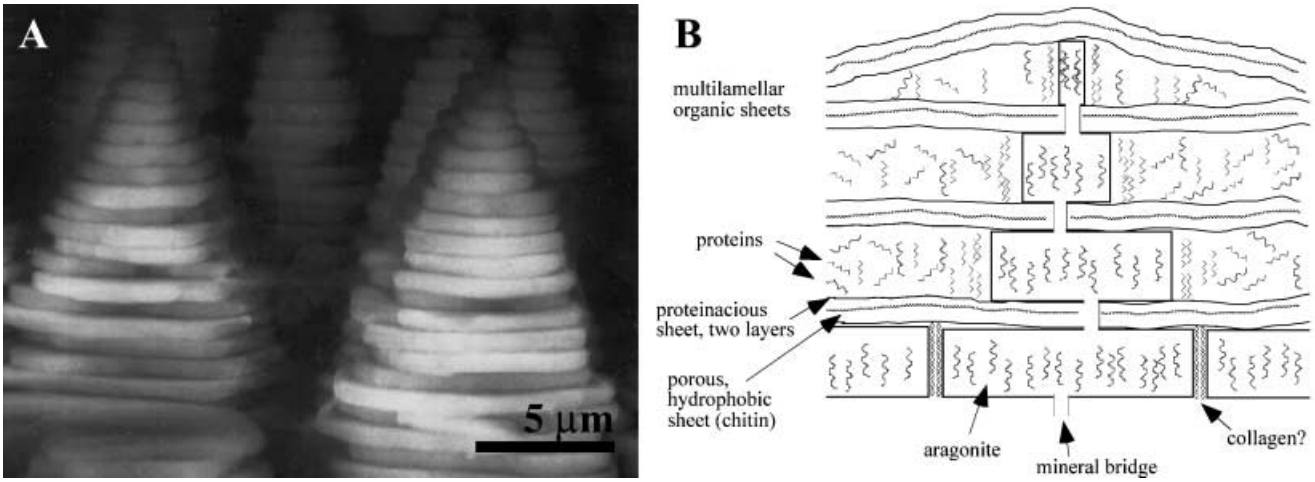

Fig. 1. (A) Scanning electron microscopy image of the growth front of nacre. The aragonite tablets appear as 'stacks of coins', where the next layer of tablets is already nucleated without the underlying layers being confluent. The tablets then grow in the horizontal direction until the layer is closed. (B) Schematic diagram of nacre growth with mineral bridges. The material for several multilamellar sheets is sectreted first and builds up in a self-organization process to moulds for the growth of aragonite tablets. The heteroepitaxial crystal growth of aragonite tablets between the multilamellar sheets of organic molecules is guided by interactions of calcium carbonate and the mineral ions Ca2+ and CO_3^{2-} with proteins in solution. Each tablet is embedded in an organic matrix. Fenestrated sheets of the supramolecular organic matrix act as porous moulds that guide the growth of nacre layer by layer via 'mineral bridges'. These connections support the alignment of the crystallographic orientations of the different aragonite tablets.

constituents are necessary. Several calcium-binding polyanionic proteins have been isolated from shells of the gastropod *Haliotis* (Nakahara *et al.*, 1982; Cariolou & Morse, 1988) and other molluscs (Weiner & Hood, 1975; Greenfield & Crenshaw, 1990; Kawaguchi & Watabe, 1993), but the strong overall negative charge of these proteins makes their characterization rather difficult. Therefore, only few proteins of nacre have been analysed on the molecular level. Most of these proteins have been discovered only very recently. Nacrein isolated from the nacre of oyster (*Pinctada fucata*) was the first protein of a molluscan shell to be sequenced and showed carbonic anhydrase and calcium-binding activity (Miyamoto *et al.*, 1996). Lustrin A from the nacre of *Haliotis rufescens* is a multidomain protein and seems to be one of the elastomeric adhesive proteins connecting the aragonite tablets and hindering the propagation of cracks (Shen *et al.*, 1997; Smith *et al.*, 1999). A family of small, acid proteins (16 kDa, pI approximately 5) named N16 or pearlin induce the formation of platy aragonite layers *in vitro* similar to the nacreous layers (Samata *et al.*, 1999; Miyashita *et al.*, 2000). This seems to be the case for N66, a nacrein homologue, and N14, another member of the N16 family (Kono *et al.*, 2000). Mucoperlin was the first reported mineralizing protein with mucin character (Marin *et al.*, 2000). Most recently, two water-soluble non-acidic proteins, perlucin and perlustrin, were isolated from abalone (*Haliotis laevigata*) nacre. Perlucin is a functional C-type lectin showing a Ca^{2+}-dependent carbohydrate binding activity with galactose and mannose specificity (Mann *et al.*, 2000). In precipitation assays (Wheeler *et al.*, 1981) with saturated calcium carbonate solution perlucin also shows nucleating activity (Weiss *et al.*, 2000). Perlustrin is homologous to the N-terminal domain of mammalian insulin-like growth factor binding proteins (Weiss *et al.*, 2001).

Atomic force microscopy (AFM) has proved to be useful in observing protein–mineral interaction directly and is a suitable method to determine how particular matrix proteins affect crystal growth. A mixture of soluble proteins isolated from *Haliotis* shell altered crystal shape and the kinetics of crystal growth and adhere preferentially to crystal steps (Walters *et al.*, 1997). A family of nacre proteins from the same organism induced the transition from calcite to aragonite growth (Thompson *et al.*, 2000).

We have used scanning electron microscopy (SEM) and AFM in combination with new preparation methods to gain novel insights into the structure and growth of abalone nacre. The results are discussed with regard to the different models of crystal growth. AFM was also applied to examine the effect of perlucin on a growing calcite surface.

Materials and methods

Cleaved nacre sample preparation

The outer calcitic layer of *Haliotis laevigata* shells was removed with a grindstone using a Proxxon Minimot 40/E drilling machine (Proxxon GmbH, Niersbach, Germany). Appropriately sized nacre pieces were then cut off with a wheel. Depending on the type of investigation, the nacre probes were split with a scalpel parallel to the aragonitic layers, ground with abrasive paper, processed with acryl polishing paste, etched with 0.5 M ethylene diamine–tetra-acetic acid (EDTA) or 10% acetic acid or treated with proteinase K (600 U mL^{-1}) or chymotrypsin 90 U mL^{-1}, and protease X 50–100 U mL^{-1}.

Preparation of saturated calcium carbonate solution

A saturated calcium carbonate solution was prepared following the protocol of Hillner *et al.* (1992). Thirty to 50 mL of 100 mM $NaHCO_3$ was added dropwise under permanent stirring to 120 mL of a 40 mM $CaCl_2$ solution. As soon as the solution became turbid, the addition of $CaCl_2$ was stopped and the pH was adjusted to 8.2 with 1 M NaOH. Finally, the solution was filtered sterile using a 0.22-μm filter.

A multi-supersaturated calcium carbonate solution was produced according to the methods of Kitano *et al.* (1962) from a suspension of 10 g L^{-1} $CaCO_3$ in deionized water (MilliQ, Millipore, El Paso, TX, U.S.A.). Compressed nitrogen was bubbled through the suspension overnight. Undissolved $CaCO_3$ was removed by sterile filtering. The solution was now ready for instant use. For aragonite crystal growth studies, 53 mM $MgCl_2$ was added before addition of nitrogen.

Preparation of saturated calcium carbonate solution with 100 mM NaCl and precipitation assay for perlucin enrichment

Twenty millimolar $CaCl_2$ in 5 mM HEPES buffer, pH 8.2, was poured into 20 mM $NaHCO_3$ in 5 mM HEPES buffer, pH 8.2, to create the saturated $CaCO_3$ solution. Sodium chloride and purified perlucin were added to a final concentration of 100 mM and 0.1 mg mL^{-1} perlucin, respectively. The control measurements were performed by adding deionized water instead of perlucin solution. If a precipitate formed the solution was centrifuged in an Eppendorf centrifuge at 1200 ***g***. The supernatant was stored and the pellet was washed with 5 mM HEPES buffer, pH 8.2, and centrifuged again at 1200 ***g***. This procedure was repeated five times. At the last step the pellet was dissolved in 10% acedic acid and the solution was applied to a sodium dodecyl sulphate polyacrylamide gel electrophoresis (SDS-PAGE) system using a 10–20% gradient Bio-Rad Ready-Gel system for visualization of intracrystaline proteins.

Isolation, purification and N-terminal sequencing of perlucin

Shells of the species *Haliotis laevigata* were obtained from the Australian Abalone Exports Pty. Ltd (Victoria, Australia). For preparation of nacre (mother of pearl) the shells were sand blasted to remove the calcitic part completely. The aragonitic fraction was rinsed with 25 mM Tris buffer, pH 7.4, cracked in a bench vice and placed into a dialysis tubing (Visking Typ 8/

32 Roth, cut-off 15 kDa, Karlsruhe, Germany) filled with the same buffer. One end of the tubing was not closed but was connected to a tube for collection of the overflow. The following steps were carried out at 4 °C. By addition of 10% acetic acid, the solution began to develop foam resulting from the release of carbon dioxide. The overflow of the foaming solution was collected until foaming stopped. By changing the dialysis buffer against fresh 10% acetic acid, the foaming started again and the overflow was collected in a second tube. In this way six fractions of 4–40 mL of foam raw extract were obtained in 1 week. The foam fractions and the remaining suspension were centrifuged at 5445 ***g*** for 50 min at 4 °C. The supernatants were dialysed against three changes of 30 volumes of 25 mM Tris, pH 7.4, 0.002% NaN_3, sterilized by filtration through a 0.22-μm filter and stored at 4 °C. Ion exchange chromatography was performed using a Pharmacia CM-Sepharose Fast Flow HiTrap column with a linear gradient of 0–1 M NaCl in 25 mM citrate buffer, pH 5.0, for 20 min at a flow rate of 1 mL min^{-1}. Protein fractions were concentrated in a speed vac concentrator and analysed by SDS-PAGE using a 10–20% gradient Bio-Rad Ready-Gel system. N-terminal amino acid sequence analysis was performed using a PE-Applied Biosystems Procise sequencer model 473A after desalting of the samples with the ProSorb device (PE-Applied Biosystems) or after reversed phase HPLC.

AFM imaging

Imaging was performed with a Nanoscope IIIa Multimode (Digital Instruments, Santa Barbara, CA, U.S.A.). Growth and dissolution studies of the geological calcite surfaces were performed in contact mode. Silicon nitride cantilevers (Microlevers, Park Scientific Instruments, Sunnyvale, CA, USA) with oxide-sharpened tips and a thickness of 0.6 μm and a force constant of 0.03 N m^{-1} were used. Cantilevers were treated with UV light for 10 min to destroy organic contaminants on the tip. The glass fluid cell and the O-ring were cleaned with a specific detergent ('Ultra Joy', Procter & Gamble, U.S.A.), rinsed thoroughly with water and blown dry with compressed nitrogen. Depending on the studies, freshly deionized water (MilliQ), saturated calcium carbonate solution with or without 0.1 mg mL^{-1} perlucin was injected with a 1-mL syringe (Injekt 40 SOLO, Braun Melsungen AG, Melsungen, Germany) into the fluid cell. To avoid air bubbles, the solutions were warmed and cooled again to room temperature. Imaging was done with an image force of about 0.5–1 nN. The scan size of the images taken with the 'J'-scanner ranged between 1 μm and 10 μm. They were taken at scan rates of 4 Hz with 512 lines per image.

SEM imaging

Suitable nacre probes cleaved parallel to the aragonite tablet layers were incubated in supersaturated calcium carbonate solution with 53 mM $MgCl_2$ for 5 days. The samples were then blown dry with compressed nitrogen. The chosen magnesium concentration corresponds to that of seawater and promotes the growth of the aragonite phase of calcium carbonate. Additional investigations concentrated on the quantitative analysis of the microstructure and provide the basis for the interpretation and modelling of the mechanical properties of nacre.

SEM investigations were performed with a Jeol JSM-5900LV (Jeol Ltd, Akishima, Japan) at high vacuum. The nacre probes were sputter-coated with gold for 50 s with a current of 32 mA in a 0.1-mbar argon atmosphere. Sputtering was performed with a Bal-Tec SCD005 (Bal-Tec AG, Balzers, Liechtenstein) yielding a gold coat of 0.7 nm thickness.

Results and discussion

The biogenic formation of the polymer/mineral composite nacre (mother of pearl) is a self-organizing process, in which organic molecules such as proteins and polysaccharides form a highly organized structure together with the calcium carbonate polymorph aragonite. Different families of proteins are thought to guide nucleation, concentration and growth of the mineral to form this high-performance material (Treccani *et al.*, 2003). Here we report on direct observations of native interlamellar organic sheets and purified proteins therefrom with the AFM, structural studies with the SEM, crystal growth studies of these interlamellar organic sheets and report on functional and biochemical studies of the water-soluble protein perlucin.

AFM imaging of the interlamellar organic sheet

In AFM the imaging tip is in mechanical contact with the sample. One major advantage of AFM imaging is the possibility to image in aqueous solution (Drake *et al.*, 1989). Not only do biological structures remain fully hydrated and native but there is also the possibility to observe dynamic processes (Radmacher *et al.*, 1994; Bezanilla *et al.*, 1994; Rief *et al.*, 1997; van Noort *et al.*, 1998; Müller *et al.*, 1999).

Freshly cleaved nacre appears in most cases to be separated between the mineral tablets and the protein layer of the multilamellar sheet (Fig. 2A,B). The surface shows a honeycomb-like pattern on the micrometre scale; these honeycombs have a diameter of about 10 μm. The honeycombs seem to be the imprint of the pseudohexagonal aragonite tablets. The pseudohexagonal walls of the honeycomb-like pattern form the walls of a mould, which is built by long filaments, running over the surface and crossing each other. The length of the filaments is much larger than one mould and the filaments are straight, rarely bent over the surface (Fig. 2C,D). The height of the walls is about 250 nm, suggesting that they have collapsed, because the aragonite tablets have a height of about 500 nm. In light microscopy images the honeycomb-like pattern is also visible and it has been shown previously that the filamentous walls can be degraded by subtilisin. The

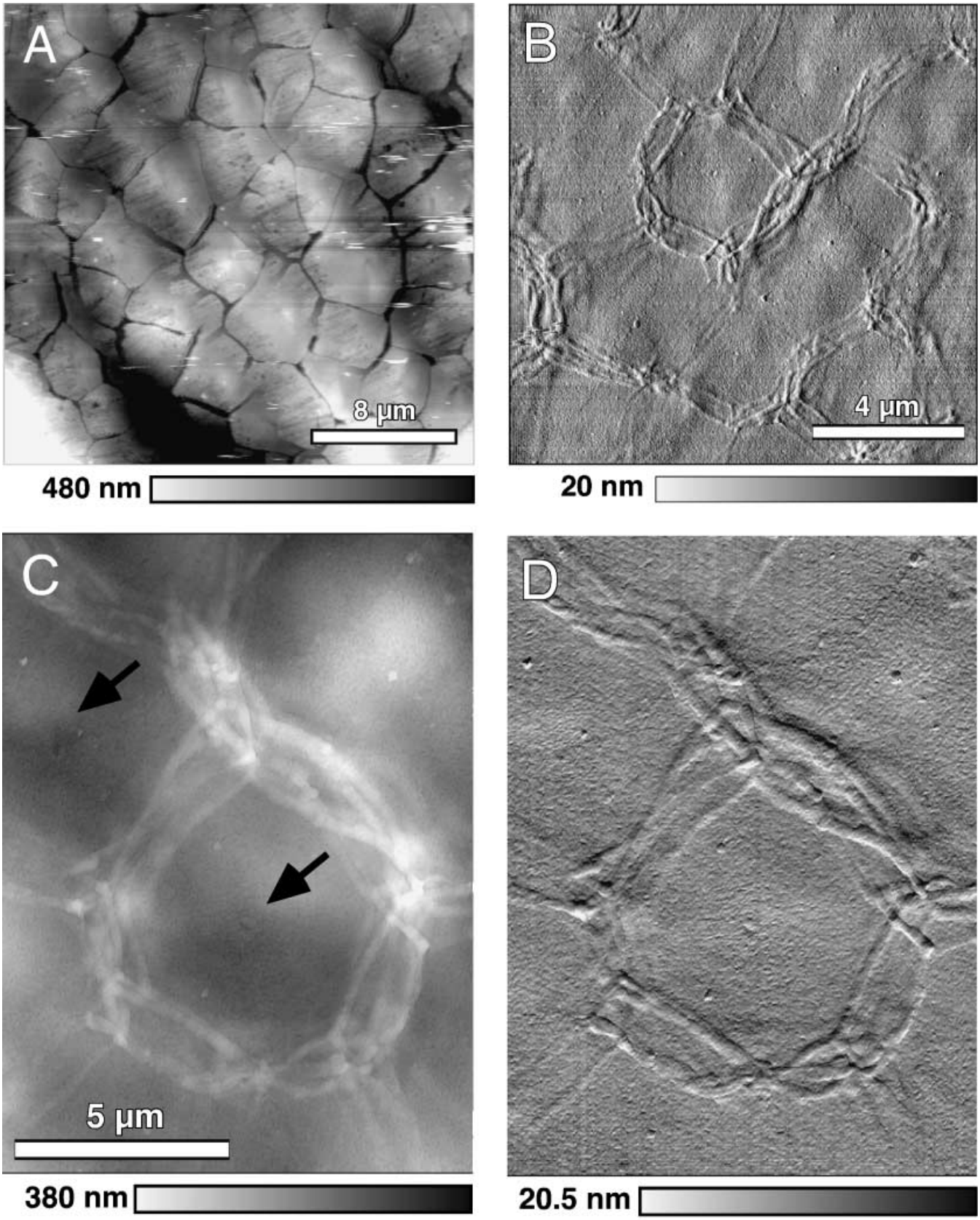
A
8 µm
480 nm
B
4 µm
20 nm
C
5 µm
380 nm
D
20.5 nm

degradation products consist mainly of glycine and proline, the major building blocks of collagen. The diameter of the filaments is approximately 50 nm, which is in good agreement with the diameter of collagen fibres.

Imaging the flat area of the mould with higher resolution reveals a pattern of tightly packed globular molecules a few nanometres in size (Fig. 3A,B). These molecules can be degraded by proteinase K, proving that they are proteins (Schäffer *et al.*, 1997). These protein sheets play an important role in the formation and alignment of aragonite, as discussed in the next paragraph. The protein molecules are attached to a filamentous network of chitin (Weiss *et al.*, 2002), which is located in the middle of the interlamellar sheet (Fig. 1). Because this chitin network is very hydrophobic and is preformed together with the proteinacious sheets as moulds into which the mineral ions are secreted, holes in the network are necessary for the secreted ions to permeate. These small holes are clearly visible in the AFM images in Fig. 3(C,D). The holes have a diameter of 50 nm leaving enough space for the rapid diffusion of ions.

In the centre of the flat part of the mould a larger hole is visible with a diameter of about 150 nm (arrows in Fig. 2C and Fig. 3C). This hole is present in the middle of each mould of those samples that have been treated with EDTA, suggesting that there has been a mineral stencil in the hole and supporting the theory of vertical mineral bridges between aragonite tablets. It has been shown previously that vertical successive aragonite layers (formed by confluent aragonite tablets) have the same crystal orientation, even though they are separated by interlamellar organic sheets (Zaremba *et al.*, 1996). Heteroepitaxial growth has been postulated (Bevelander & Nakahara, 1969; Nakahara, 1979; Morse *et al.*, 1993), in which proteins act as mediators of the crystal lattice from one mineral layer to the next. This would then lead to a continuous crystal over several (or all) mineral layers. A different hypothesis has recently been suggested: mineral bridges between each layer (Schäffer *et al.*, 1997). Abalone nacre may instead be formed by continuous growth through pores or holes in the interlamellar organic sheet and the information from the crystal lattice is passed on to the next layer by uninterupted growth. Our findings support the latter hypothesis, although definitive ultimate proof is still missing, i.e. imaging the mineral bridge itself. This will be the aim of future work.

SEM imaging of aragonite formation on interlamellar sheets and on nacre mineral

Scanning electron microscopy is one of the key tools in investigating the structure of nacre. The mineral part of nacre can be observed from the millimetre to micrometre scale and the results obtained have provided detailed information on the mineral structure (Wada, 1972; Nakahara, 1983; Zaremba *et al.*, 1996; Evans *et al.*, 2001). This information needs to be considered when modelling the strain and failure behaviour of nacre. Figure 4 illustrates the particular stacking of aragonite tablets in native nacre. In contrast to technical ceramics, in which their microstructures are originated by high-temperature processes, nacre is characterized by effective self-organization synthesis, which leads to the unique microstructure of this biogenic composite. Deformation, crack initiation and propagation are investigated at different hierachical levels, from micromechanical experiments up to the measurement of standardized materials test data.

We used SEM for imaging overgrowth experiments of crystals from supersaturated calcium carbonate solution on differently treated cleavage surfaces of nacre. When untreated, freshly cleaved nacre was incubated with supersaturated calcium carbonate solution, tightly packed needles of aragonite crystals (Feigel stain) grew on the surface. These needles were perfectly aligned perpendicular to the nacre surface (Fig. 5A,B). On freshly cleaved nacre surfaces, where the proteinacous part was removed by proteinase K, no growth of perpendicular orientated needles was observed, but a few bundles of aragonite needles grew on some steps of the nacre surface (Fig. 5C). This might be due to some remnants of proteins at those steps. With these experiments it is clear that the protein layer of the interlamellar sheet favours the growth of aragonite. On the protein layer the crystals grown from solution grow in single needles, instead of bundles of needles in the absence of the protein layer. The needles are growing in the *c*-direction (001), which is the fast direction of crystal growth in aragonite. In nacre the *c*-direction might also be the fast growth direction, but it is the direction of least crystal extension (about 0.5 μm vs. about 10 μm in the *a*- and *b*-directions). The factors responsible for this behaviour lay either in a form of contact stop of growth of the following organic layer in nacre or in the water-soluble (possibly inhibitory) proteins present in the growth solution in the moulds for the aragonite tablets in growing nacre. In light of our hypothesis that several consecutive layers of nacre grow as a single crystal through mineral bridges, the protein layer of the interlamellar sheet could support the uninteruppted growth through a mineral bridge.

AFM imaging of growth and dissolution of calcite and the interaction of perlucin with those surfaces

AFM has been used to observe growth and dissolution of

Fig. 2. (A) AFM image (contact mode in air) of nacre after polishing and etching with 0.5 M EDTA. The dense packing of polygonal aragonite tablets with a diameter of 5–10 μm is clearly visible. (B) AFM deflection image of nacre ground parallel to the aragonite layers and 1 h incubation in 10% acetic acid. The organic matrix shows a hole above each aragonite tablet with a diameter of 150 nm. Additional structural elements are twisted proteinaceous filaments that form a network along the interspace between the aragonite tablets. These filaments extend along several tablets and cross each other or end at the edges of the tablets. (C) Enlargement of B. Black arrow points to the hole in the organic sheet in the middle of each aragonite tablet. (D) Deflection image of C.

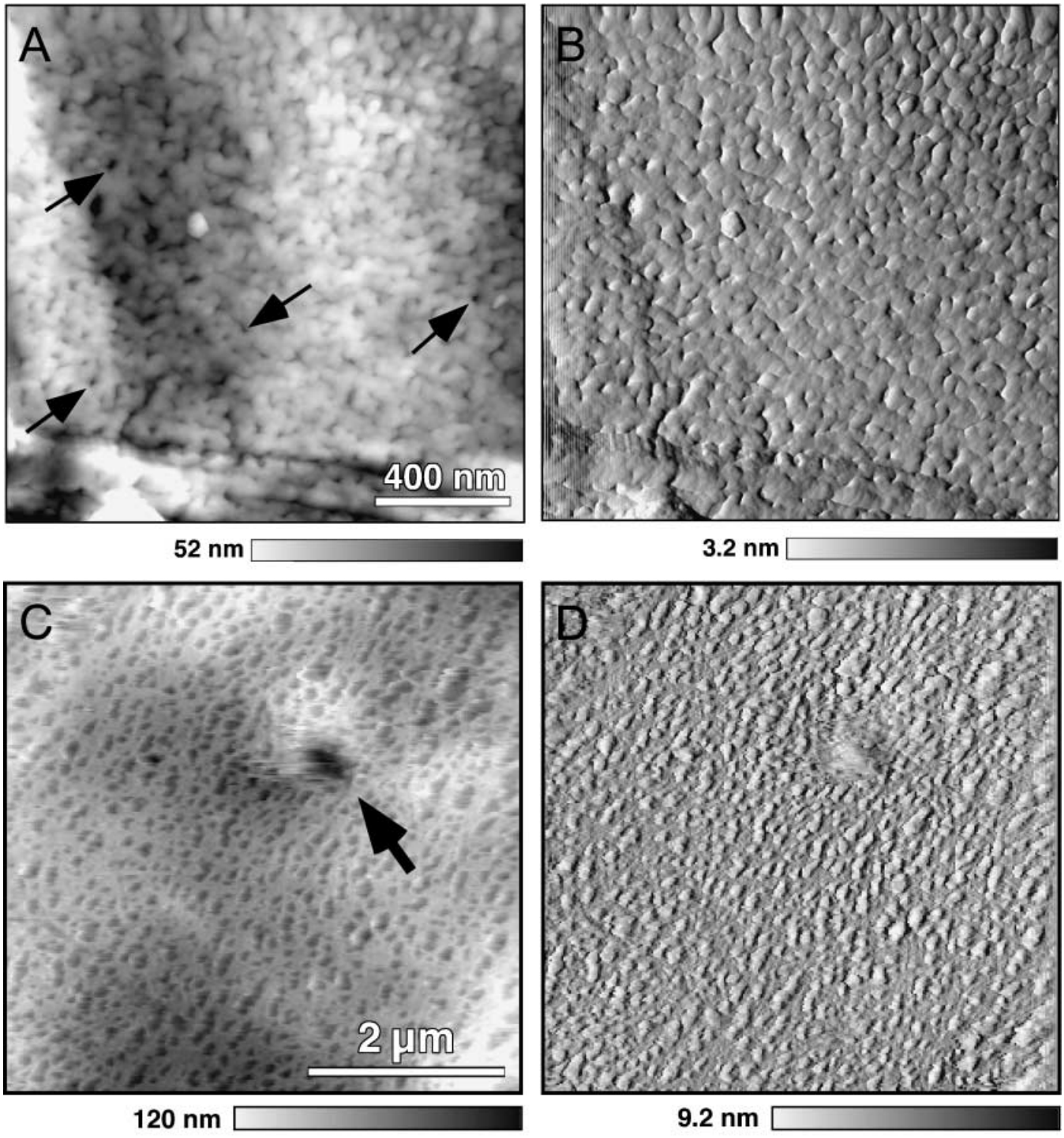

Fig. 3. (A) AFM images (contact mode in air, height and deflection images) of demineralized multilamelar organic sheets. The structure appears as an irregular fibrous network with pores (black arrows) of 40–80 nm diameter. (B) Deflection image of A. (C) AFM image of the organic matrix after 2 h incubation with proteinase K (600 U mL^{-1}) in Tris buffer, pH 7.5. After 15 min the proteins are degraded and the size of the pores and the hole in the middle increase. A fibrous network of chitin is visible. (D) Deflection image of C.

calcite directly (Hillner *et al.*, 1992) and it has been used to examine the interaction of a mixture of nacre-extracted proteins with the mineral phase (Walters *et al.*, 1997; Thompson *et al.*, 2000). In these experiments the proteins induced aragonite growth on top of a calcite crystal. We used the AFM to image the interaction of purified perlucin (Mann *et al.*, 2000) with the calcite surface. During AFM imaging the sharp tip is in mechanical contact with the sample. One of the most

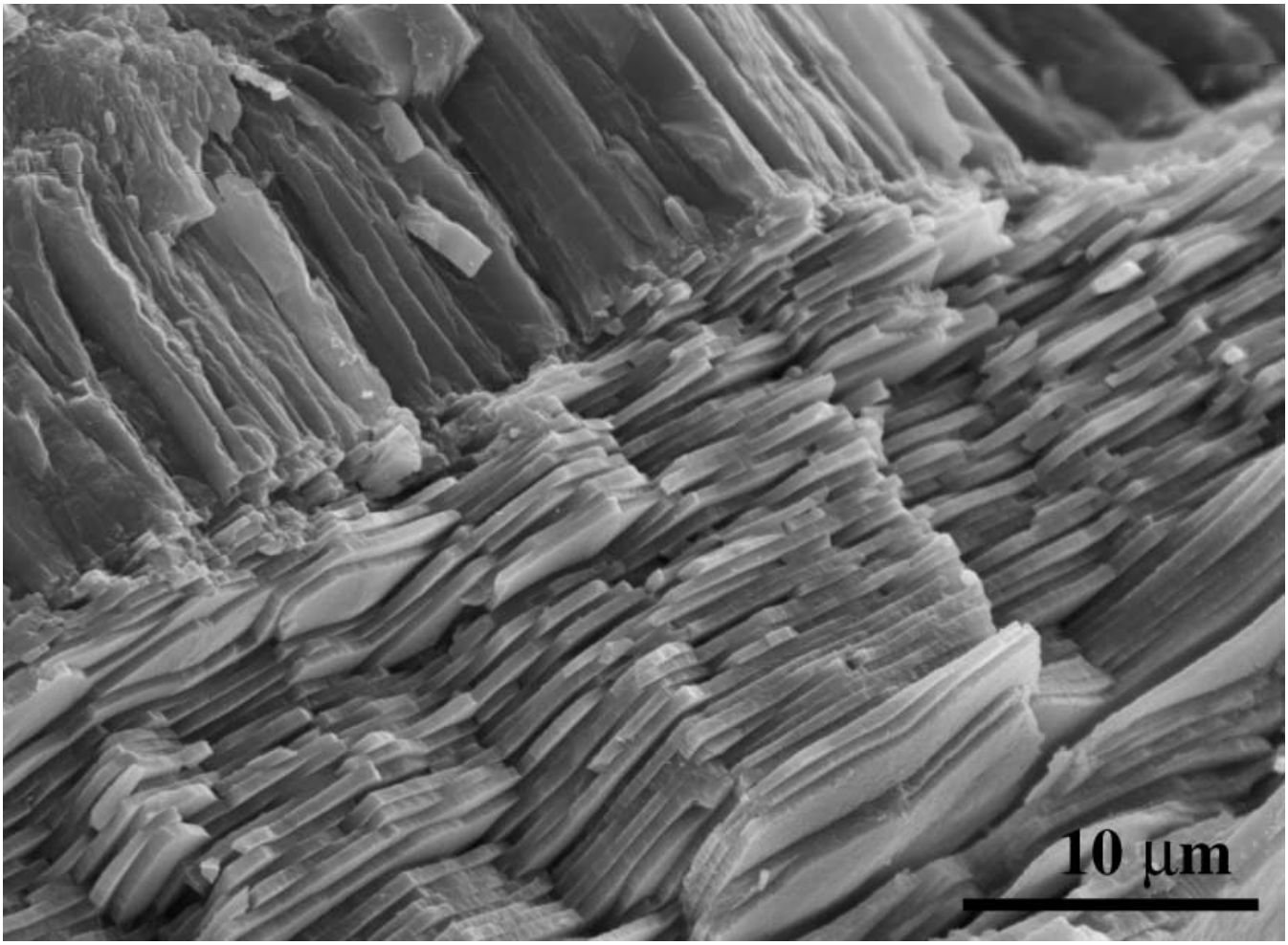

Fig. 4. SEM micrograph of a fracture surface of nacre (right lower half of image) and calcite (left upper half) illustrating the stacking of aragonite tablets.

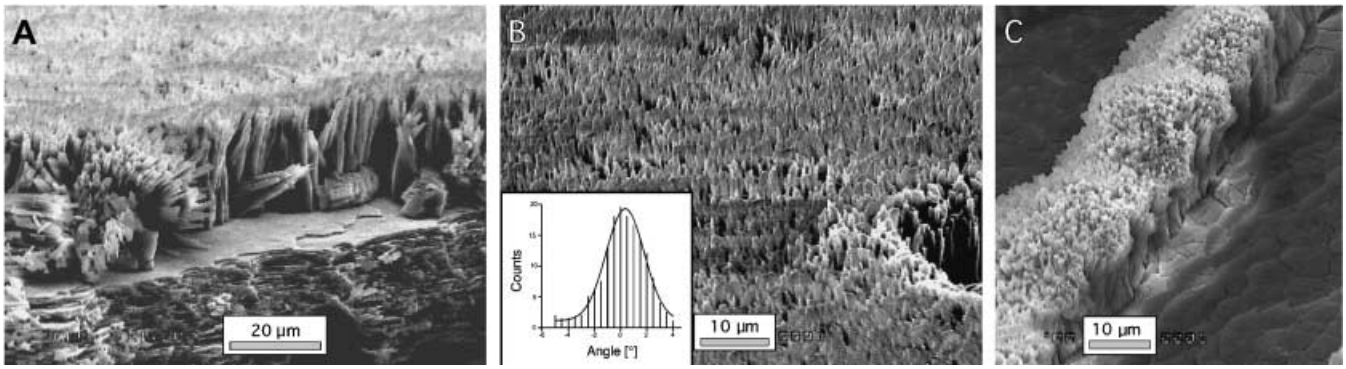

Fig. 5. (A) SEM image of tighly packed aragonite needles grown on a cleaved, native nacre surface facing towards the inside of the shell. The needles are orientated perpendicular to the surface and parallel to the crystallographic *c*-direction (001). (B) SEM image of aragonite needles grown on cleaved nacre surface facing the outside of the shell. The surface is covered with a highly orientated layer of aragonite needles. The distribution of tilt angles from a random group of needles can be approximated with a gaussian distribution (inset). (C) SEM image of aragonite needles grown on cleaved nacre after 3 days incubation with chymotrypsin (900 U mL^{-1}) and protease typ X (50–100 U mL^{-1}). Needle bundels grow in separate bunches or along edges.

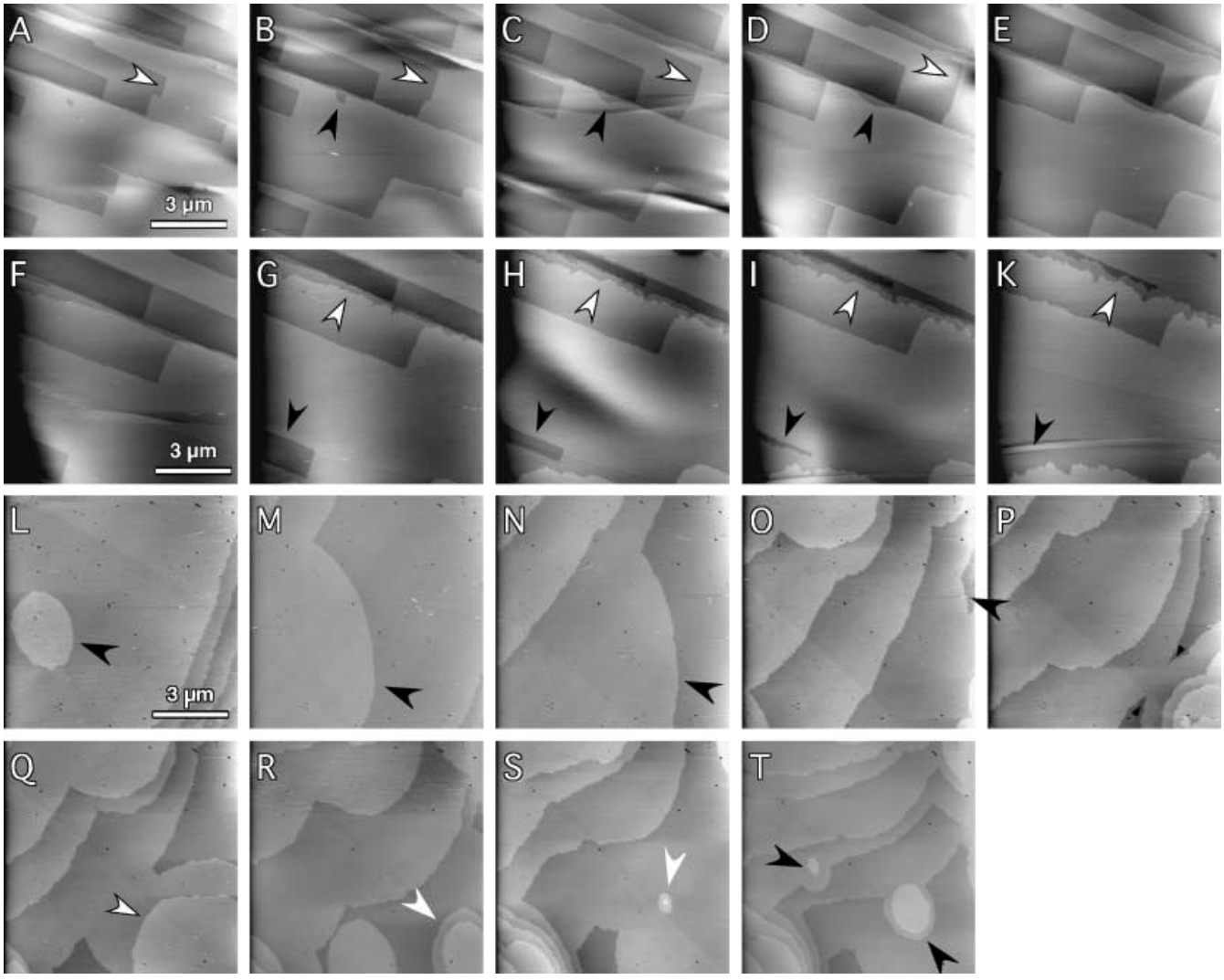

Fig. 6. AFM measurements of the interaction of perlucin with geological calcite (3-min interval between two images). (A–E) Consecutive AFM images of a ($4\overline{41}$) calcite surface immersed in deionized water. The calcite crystal slowly desolves layer by layer (white and black arrowheads). (F–K) Consecutive AFM images of the growth of calcite ($4\overline{41}$) surface in saturated calcium carbonate solution. Note the growth of the molecular layers (white and black arrowheads). (L–T) Consecutive AFM images show a ($4\overline{41}$) calcite surface immersed in saturated calcium carbonate solution with perlucin (0.01 mg mL^{-1}). Note that perlucin nucleates small islands (e.g. R, S, light grey arrowheads) for the next molecular layer. As different layers (e.g. L to O, black arrowheads) merge without detectable defects (e.g. small arrowheads in P), it is reasonable to suggest that perlucin induces epitactic growth of new layers in the orientation of the crystal lattice.

important features of our AFM is the fluid cell. When imaging a calcite crystal it can be immersed in aqueous solution and the solution can be exchanged during imaging or even be continuously exchanged.

Figure 6 shows results of experiments in which the surface of a $4\overline{41}$ face has been imaged under different conditions. In the first row of Fig. 6(A–E) the dissolution of the calcite crystal from the $4\overline{41}$ face is shown. The single crystal layers in this face, comprising alternating CO_3^{2-} and Ca^{2+} ions, are visible. The steps that terminate each layer are straight. When deionized water is added, the steps are slowly degraded (Fig. 6A–D, white arrowheads), and the crystal dissolves at the steps leaving the steps straight, except for small corrugations (Fig. 6B–D, black arrowheads), probably at areas of defects in the crystal.

In the second row of Fig. 6(F–K) the same crystal surface (face) grows as saturated calcium carbonate solution is added to the sample. The layers grow quickly and the steps are therefore more corrugated on the nanometre scale (Fig. 6G–K, white arrowheads) but appear straight on the micrometre scale (Fig. 6G–K, black arrowheads). The different layers become confluent and the surface of the calcite crystal become flatter the longer the saturated calcium carbonate solution was present (Fig. 6K).

In the third and forth rows of Fig. 6(L–T) saturated calcium carbonate solution with 0.1 mg mL^{-1} of purified perlucin is

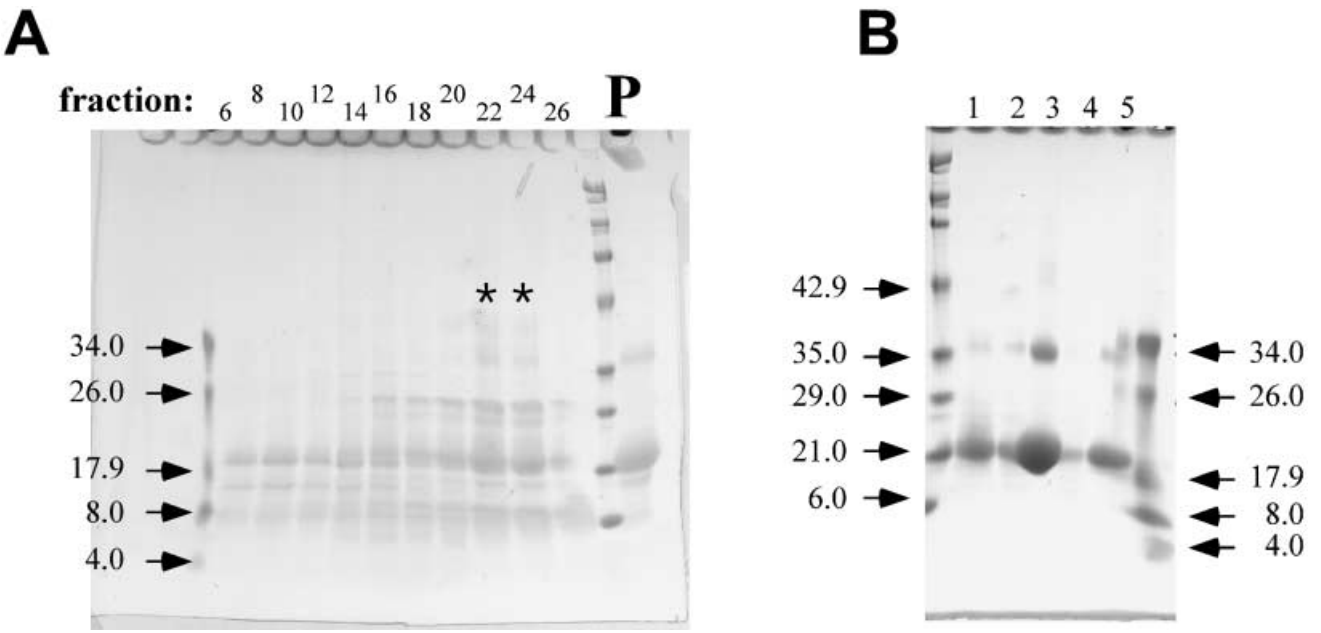

Fig. 7. SDS-PAGE of water-soluble proteins of nacre after anion exchange chromatography and precipitation experiments of perlucin with calcium carbonate crystals. (A) SDS-PAGE after chromatographic isolation of the water-soluble protein fraction. Fractions with asterisks were used for precipitation experiments of calcium carbonate crystals from saturated solution with perlucin. (B) SDS-PAGE of precipitate after dissolution of the mineral crystal. It shows that pure perlucin (lane 3) precipitates with calcium carbonate crystals.

incubated on the same crystal surface (face). At the beginning of this experiment the surface is flat (healed out), because of treatment with saturated calcium carbonate solution. A new roundish layer (Fig. 6L, black arrowhead) is visible in the middle of a flat layer. This roundish layer grows with time (Fig. 6M–O, black arrowheads) and finally becomes confluent with another layer nucleated at another site (Fig. 6P, black arrowhead). At the line at which those two layers become confluent (Fig. 6P, small arrowheads) there is no defect detectable, suggesting that the newly nucleated layers are nucleated by perlucin epitactically at the orientation of the underlying crystal lattice. In the subsequent images, more layers are nucleated (Fig. 6Q, white arrowhead). On top of the new layers other new layers appear (Fig. 6R–T, pale grey arrowheads).

These experiments show clearly that perlucin is a nucleating protein, although the related protein lithostatin (Bertrand *et al.*, 1996) in mammals is thought to be an inhibitor of crystal growth (Multigner *et al.*, 1983). We show below that perlucin can be incorporated into calcium carbonate crystals.

Precipitation experiments of calcium carbonate solutions with nacre proteins

Saturated calcium carbonate solution was used for the precipitation experiments with perlucin. In former experiments we have shown that perlucin accelerates the nucleation phase of precipitating calcium carbonate solution (Weiss *et al.*, 2000). Using a hydrophobic surface (Teflon) the precipitating crystals grew in a dendritic fashion if the solution contained perlucin.

This highly specific interaction of perlucin with CO_3^{2-} or Ca^{2+} ions or $CaCO_3$ can be used to purify perlucin from the water-soluble, nacre protein mixture. The water-soluble protein fraction of nacre was prepurified by anion exchange chromatography (Fig. 7A). Fraction 22–24 (Fig. 7A, asterisks) of the sodium chloride gradient was dialysed against saturated calcium carbonate solution with 100 mM NaCl. Small crystals precipitated from the solution in the dialysis tubing. After two changes the solution in the tubing was collected and centrifuged. The supernatant was collected and the pellet was washed in HEPES buffer, pH 8.2, several times. The pellet consisted of small white cystals, which did not dissolve in the buffer solution but dissolved immediately in 10% acedic acid. The dissolved pellet was analysed by SDS-PAGE (Fig. 7B, lane 3) and showed that it contained pure perlucin, which was identified by N-terminal sequencing of the protein. This experiment shows that perlucin became incorporated into calcium carbonate crystals, creating a first small protein/mineral composite fabricated *in vitro*.

Conclusions and outlook

We have shown that the proteins in the polymer/mineral composite nacre guide nucleation and growth of the mineral phase. These proteins are also responsible for the mechanical properties of nacre, giving a fracture strength that is three

orders of magnitude larger than for the pure mineral. Although comprising only 5% in nacre, the organic material forms moulds for the mineral crystals, which consist of honeycomb-like structures forming imprints for the pseudohexagonal aragonite tablets. Proteins in the multilamellar organic sheet act as templates for the growth of aragonite crystals, whereas pores in the hydrophobic core of the multilamellar organic sheet might guide mineral bridges between the aragonite layers. The purified nacre protein perlucin nucleates calcium carbonate crystals and becomes incorporated into these crystals in the presence of sodium chloride. This information needs to be considered when modelling the micromechanical properties of nacre. Moreover, this information may provide the basis for creating new functional ceramic composites through biomineralization.

Acknowledgements

We thank Manfred Radmacher for helpful discussions and his kind support. This work was supported by the Deutsche Forschungsgemeinschaft (S.B., S.K., L.T., M.A., M.F.).

References

Addadi, L. & Weiner, S. (1985) Interactions between acidic proteins and crystals: stereochemical requirements in biomineralisation. *Proc. Natl Acad. Sci. USA*, **82**, 4110–4114.

Belcher, A.M., Wu, X.H., Christensen, R.J., Hansma, P.K., Stucky, G.D. & Morse, D.E. (1996) Control of crystal phase switching and orientation by soluble mollusc-shell proteins. *Nature*, **381**, 56–58.

Berman, A., Hanson, J., Leiserowitz, L., Koetzle, T.F., Weiner, S. & Addadi, L. (1993) Biological control of crystal texture: a widespread strategy for adapting crystal properties to function. *Science*, **259**, 776–779.

Bertrand, J.A., Pignol, D., Bernard, J.-P., Verdier, J.-M., Dagorn, J.-C. & Fontecilla-Camps, J.C. (1996) Crystal structure of human lithostatine, the pancreatic inhibitor of stone formation. *EMBO J.* **15**, 2678–2684.

Bevelander, G. & Nakahara, H. (1969) An electron microscope study of the formation of the nacrous layer in the shell of certain bivalve molluscs. *Calc. Tiss. Res.* **3**, 84–92.

Bezanilla, M., Drake, B., Nudler, E., Kashlev, M., Hansma, P.K. & Hansma, H.G. (1994) Motion and enzymatic degradation of DNA in the atomic force microscope. *Biophys. J.* **67**, 1–6.

Borbas, J.E., Wheeler, A.P. & Sikes, C.S. (1991) Molluscan shell matrix phosphoproteins: correlation of degree of phosphorylation to shell mineral microstructure and to in vitro regulation of mineralization. *J. Exp. Zool.* **258**, 1–13.

Cariolou, M.A. & Morse, D.E. (1988) Purification and characterization of calcium-binding conchiolin shell peptides from the mollusc, *Haliotis rufescens*, as a function of development. *J. Comp. Physiol. B*, **157**, 717–729.

Currey, J.D. (1980) Mechanical properties of mollusc shell. *The Mechanical Properties of Biological Materials* (ed. by J. F. V. Vincent and J. D. Currey), pp. 75–97. Cambridge University Press, Cambridge, U.K.

Drake, B., Prater, C.B., Weisenhorn, A.L., Gould, S.A.C., Albrecht, T.R., Quate, C.F., Cannell, D.S., Hansma, H.G. & Hansma, P.K. (1989) Imaging crystals, polymers, and processes in water with the atomic force microscope. *Science*, **243**, 1586–1589.

Erben, H.K. (1974) On the structure and growth of the nacreous tablets in gastropods. *Biomineralization*, **1**, 14–27.

Evans, A.G., Suo, Z., Wang, R.Z., Aksay, I.A., He, M.Y. & Hutchinson, J.W. (2001) Model for the robust mechanical behaviour of nacre. *J. Mater. Res.* **16**, 2475.

Falini, G., Albeck, S., Weiner, S. & Addadi, L. (1996) Control of aragonite or calcite polymorphism by mollusk shell macromolecules. *Science*, **271**, 67–69.

Fritz, M., Belcher, A.M., Radmacher, M., Walters, D.A., Hansma, P.K., Stucky, G.D., Morse, D.E. & Mann, S. (1994) Flat pearls from biofabrication of organized composites on inorganic substrates. *Nature*, **371**, 49–51.

Fritz, M. & Morse, D.E. (1998) The formation of highly organized biogenic polymer/ceramic composite materials: the high-performance microaluminate of molluscan nacre. *Curr. Opin. Cell Biol.* **3**, 55–62.

Greenfield, E.M. & Crenshaw, M.A. (1990) Mineral induction by the soluble matrix from molluscan shells. *Origin, Evolution, and Modern Aspects of Biomineralisation in Plants and Animals* (ed. by R. E. Crick), pp. 303–307. Plenum Press, New York.

Hillner, P.E., Gratz, A.J., Manne, S. & Hansma, P.K. (1992) Atomic scale imaging of calcite growth and dissolution in real tim. *Geology*, **20**, 359–362.

Kawaguchi, T. & Watabe, N. (1993) The organic matrices of the shell of the American oyster *Crassostrea virginica* Gmelin. *J. Exp. Biol. Ecol.* **170**, 11–27.

Kitano, Y., Park, K. & Hood, D.W. (1962) Pure aragonite synthesis. *J. Geophys. Res.* **67**, 4873–4874.

Kono, M., Hayashi, N. & Samata, T. (2000) Molecular mechanism of the nacreaus layer formation in *Pinctada maxima*. *Biochem. Biophys. Res. Comm.* **269**, 213–218.

Mann, K., Weiss, I.M., Andre, S., Gabius, H.-J. & Fritz, M. (2000) The amino acid sequence of the abalone (*Haliotis laevigata*) nacre protein perlucin. Detection of a functional C-type lectin domain with galactose/mannose specificity. *Eur. J. Biochem.* **267**, 5257–5264.

Marin, F., Corstjens, P., De Gaulejac, B., De Vrind-De Jong, E. & Westbroek, P. (2000) Mucins and molluscan calcification. *J. Biol. Chem.* **275**, 20667–20675.

Miyamoto, H., Miyashita, T., Okushima, M., Nakano, S., Morita, T. & Matsushiro, A. (1996) A carbonic anhydrase from the nacreous layer in oyster pearls. *Proc. Natl Acad. Sci. USA*, **93**, 9657–9660.

Miyashita, T., Takagi, R., Okushima, M., Nakano, S., Miyamoto, H., Nishikawa, E. & Matsushiro, A. (2000) Complementary DNA cloning and characterization of pearlin, a new class of matrix protein in the nacreous layer of oyster pearls. *Mar. Biotechnol.* **2**, 409–418.

Moradian-Oldak, J., Frolow, F., Addadi, L. & Weiner, S. (1992) Interactions between acidic matrix macromolecules and calcium phosphate ester crystals: relevance to carbonate apatite formation in biomineralization. *Proc. R. Soc. Lond. B*, **247**, 47–55.

Morse, D.E., Cariolou, M.A., Stucky, G.D., Zaremba, C.M. & Hansma, P.K. (1993) Genetic coding in biomineralization of microlaminate composites. *Mat. Res. Soc. Symp. Proc.*, **292**, 59–67.

Müller, D.J., Baumeister, W. & Engel, A. (1999) Controlled unzipping of a bacterial surface layer with atomic force microscopy. *PNAS*, **96**, 13170–13174.

Multigner, L., DeCaro, A., Lombardo, D., Campese, D. & Sarles, H. (1983) Pancreatic stone protein, a phosphoprotein which inhibits calcium carbonate precipitation from human pancraetic juice. *Biochem. Biophys. Res. Commun.* **110**, 69–74.

Nakahara, H. (1979) An electron microscope study of the growing surface of nacre in two gastropode species *Turbo cornutus* and *Tegula pfeifferi*. *Venus*, **38**, 205–211.

Nakahara, H. (1983) Calcification of gastropode nacre. *Biomineralization and Biological Metal Accumulation* (ed. by P. Westbroeck and E. W. De Jong), pp. 225–230. D. Reidel Publishing Co., Dordrecht.

Nakahara, H., Bevelander, G. & Kakei, M. (1982) Electron microscopic and amino acid studies on the outer and inner shell layers of *Haliotis rufescens*. *Venus*, **41**, 33–46.

van Noort, S.J.T., van der Werf, K.O., Eker, A.P.M., de Grooth, B.G., van Hulst, N.F. & Greve, J. (1998) Direct visualization of dynamic protein–DNA interactions with a dedicated atomic force microscope. *Biophys. J.* **74**, 2840–2849.

Radmacher, M., Fritz, M., Hansma, H.G. & Hansma, P.K. (1994) Direct observation of enzyme activity with the atomic force microscope. *Science*, **265**, 1577–1579.

Rief, M., Gautel, M., Fernandez, J. & Gaub, H.E. (1997) Reversible unfolding of individual titin immunoglobulin domains by AFM. *Science*, **276**, 1109–1112.

Samata, T., Hayashi, N., Kono, M., Hasegawa, K., Horita, C. & Akera, S. (1999) A new matrix protein family related to the nacreous layer formation of *Pinctada fucata*. *FEBS Lett*. **462**, 225–229.

Schäffer, T.E., Ionescu-Zanetti, C., Proksch, R., Fritz, M., Walters, D.A., Almquist, N., Zaremba, C.M., Belcher, A.M., Smith, B.L., Stucky, G.D. *et al.* (1997) Does abalone nacre form by heteroepitaxial nucleation or by growth through mineral bridges? *Chem. Mat*. **9**, 1731–1740.

Shen, X., Belcher, A.M., Hansma, P.K., Stucky, G.D. & Morse, D.E. (1997) Molecular cloning and characterization of lustrin A, a matrix protein from shell and pearl nacre of *Haliotis rufescens*. *J. Biol. Chem*. **272**, 32472–32481.

Smith, B.L., Schäffer, T.E., Viani, M., Thompson, J.B., Frederick, N.A., Kindt, J., Belcher, A., Stucky, G.D., Morse, D.E. & Hansma, P.K. (1999) Molecular mechanistic origin of the toughness of natural adhesives, fibres and composites. *Nature*, **399**, 761–763.

Thompson, J.B., Paloczi, G.T., Kindt, J., Michenfelder, M., Smith, B.L., Stucky, G., Morse, D.E. & Hansma, P.K. (2000) Direct observation of the transition from calcite to aragonite growth as induced by abalone shell proteins. *Biophys. J*. **79**, 3307–3312.

Treccani, L., Koshnavaz, S., Blank, S., vonRoden, K., Schulz, U., Weiss, I., Mann, K., Radmacher, M. & Fritz, M. (2003) Biomineralizing proteins, with emphasis on invertebrate-mineralized structures. *Biopolymers* (ed. by Fahnestock and Steinbüchl), pp. 289–321. Wiley-VCH-Verlag GmbH, Weinheim.

Wada, K. (1972) Nucleation and growth of aragonite crystals in the nacre of some bivalve molluscs. *Biomineralization*, **6**, 141–159.

Wada, K. & Fujinuki, T. (1976) Biomineralization in bivalve molluscs with emphasis on the chemical composition of the extrapallial fluid. *The Mechanisms of Mineralisation in the Invertebrates and Plants* (ed. by N. Watabe and K. M. Wilbur), pp. 175–190. University of South Caroline Press, Columbia.

Walters, D.A., Smith, B.L., Belcher, A.M., Paloczi, G.T., Stucky, G.D., Morse, D.E. & Hansma, P.K. (1997) Modification of calcite crystal growth by abalone shell proteins: an atomic force microscope study. *Biophys. J*. **72**, 1425–1433.

Wang, R.Z., Suo, Z., Evans, A.G., Yao, N. & Aksay, I.A. (2001) Deformation mechanisms in nacre. *J. Mater. Res*. **16**, 2485.

Weiner, S. (1979) Aspartic acid-rich proteins: major components of the soluble organic matrix of mollusk shells. *Calcif. Tissue Int*. **29**, 163–167.

Weiner, S. & Addadi, L. (1997) Design strategies in mineralized biological materials. *J. Mater. Chem*. **7**, 689–701.

Weiner, S. & Hood, L. (1975) Soluble protein of the organic matrix of mollusk shells: a potential template for shell formation. *Science*, **190**, 987–988.

Weiner, S. & Traub, W. (1980) X-ray diffraction study of the insoluble organic matrix of mollusk shells. *FEBS Lett*. **111**, 311–316.

Weiss, I.M., Göhring, W., Fritz, M. & Mann, K. (2001) Perlustrin, a *Haliotis laevigata* (abalone) nacre protein is homologous to the insulin-like growth factor binding protein N-terminal module of vertebrates. *Biophys. Biochem. Res. Commun*. **285**, 244–249.

Weiss, I.M., Kaufmann, S., Mann, K. & Fritz, M. (2000) Purification and identification of perlucin and perlustrin, two new proteins from the shell of the mollusc *Haliotis laevigata*. *Biophys. Biochem. Res. Commun*. **267**, 17–21.

Weiss, I.M., Renner, C., Strigl, M.G. & Fritz, M. (2002) A simple and reliable method for the determination and localization of chitin in abalone nacre. *Chem. Mat*. **14**, 3252–3259.

Wheeler, A.P., George, J.W. & Evans, C.A. (1981) Control of calcium carbonate nucleation and crystal growth by soluble matrix of oyster shell. *Science*, **212**, 1397–1398.

Zaremba, C.M., Belcher, A.M., Fritz, M., Li, Y., Mann, S., Hansma, P.K., Morse, D.E., Speck, J.S. & Stucky, G.D. (1996) Critical transitions in the biofabrication of red abalone shells and flat pearls. *Chem. Mat*. **8**, 679–690.

Zentz, F., Bédouet, L., Almeida, M.J., Milet, C., Lopez, E. & Giraud, M. (2001) Characterization and quantification of chitosan extracted from nacre of the abalone *Haliotis tuberculata* and the oyster *Pinctada maxima*. *Mar. Biotechnol*. **3**, 36–44.